Human Molecular Genetics, 2010, Vol. 19, No. 22 **4330–4344**
doi:10.1093/hmg/ddq355
Advance Access published on August 20, 2010

The retinitis pigmentosa protein RP2 interacts with polycystin 2 and regulates cilia-mediated vertebrate development

Toby Hurd[1,*,†], Weibin Zhou[1,†], Paul Jenkins[2], Chia-Jen Liu[3], Anand Swaroop[6], Hemant Khanna[4], Jeffrey Martens[2], Friedhelm Hildebrandt[1,5] and Ben Margolis[3]

[1]Department of Pediatrics and Communicable Diseases, [2]Department of Pharmacology, [3]Department of Internal Medicine, [4]Department of Ophthalmology and Visual Sciences and [5]Howard Hughes Medical Institute, University of Michigan, Ann Arbor, MI 48109, USA and [6]Neurobiology–Neurodegeneration & Repair Laboratory (N-NRL), National Eye Institute, National Institutes of Health, Bethesda, MD 20892, USA

Received April 13, 2010; Revised July 25, 2010; Accepted August 17, 2010

Ciliopathies represent a growing group of human genetic diseases whose etiology lies in defects in ciliogenesis or ciliary function. Given the established entity of renal–retinal ciliopathies, we have been examining the role of cilia-localized proteins mutated in retinitis pigmentosa (RP) in regulating renal ciliogenesis or cilia-dependent signaling cascades. Specifically, this study examines the role of the *RP2* gene product with an emphasis on renal and vertebrate development. We demonstrate that in renal epithelia, RP2 localizes to the primary cilium through dual acylation of the amino-terminus. We also show that RP2 forms a calcium-sensitive complex with the autosomal dominant polycystic kidney disease protein polycystin 2. Ablation of RP2 by shRNA promotes swelling of the cilia tip that may be a result of aberrant trafficking of polycystin 2 and other ciliary proteins. Morpholino-mediated repression of RP2 expression in zebrafish results in multiple developmental defects that have been previously associated with ciliary dysfunction, such as hydrocephalus, kidney cysts and *situs inversus*. Finally, we demonstrate that, in addition to our observed physical interaction between RP2 and polycystin 2, dual morpholino-mediated knockdown of polycystin 2 and RP2 results in enhanced *situs inversus*, indicating that these two genes also regulate a common developmental process. This work suggests that RP2 may be an important regulator of ciliary function through its association with polycystin 2 and provides evidence of a further link between retinal and renal cilia function.

INTRODUCTION

Recent years have seen an explosion in our understanding of the diverse functions of cilia in different tissues and their role in the etiology of human disease. Cilia are highly conserved organelles both through evolution and between different cell types. They share a conserved group of proteins required for cilia formation, called the intra-flagella transport (IFT) proteins (1,2). This group of proteins, originally identified in the biflagellate *Chlamydomonas reinhardtii*, appears to function as the predominant transport mechanism for the formation and maintenance of cilia through delivery and removal of cilia proteins (3). As such, disruption of IFT through the mutation or targeted knockout of key components often results in compromised cilia function in multiple tissues. Indeed, there are a growing number of human pathologies with multi-organ phenotypes that arise from mutation in cilia-associated gene products. Two such pathologies are Bardet–Biedl syndrome (BBS) and Senior–Loken syndrome where the cystic kidney disease nephronophthisis (NPHP) is accompanied by retinal degeneration (4,5).

Primary cilia are essential for proper function of renal epithelia and retinal photoreceptor cells. Renal cilia protrude

*To whom correspondence should be addressed at: Department of Pediatrics and Communicable Diseases, University of Michigan, 1150 West Medical Center Drive, 8220 MSRBIII, Ann Arbor, MI 48109, USA. Tel: +1 7349368662; Email: twhurd@umich.edu
†These authors contributed equally to this work.

from the apical aspect of the epithelium lining the nephron and may be involved in sensing fluid flow through the nephron lumen (6). These cilia may also be essential to maintain correct orientation of individual epithelial cells within the plane of the epithelial sheet. Defects in ciliary function result in the formation of fluid-filled cysts thought to be the result of defective planar cell polarity and de-differentiation of the epithelium (7,8). In photoreceptors, the outer segment forms from the primary cilium and the cilium subsequently functions as the transition zone connecting the light sensing outer segment to the inner segment. IFT plays a key role in the shuttling of cargo between the two cellular compartments (9). Photoreceptors are highly metabolically active as they undergo periodic outer segment disc shedding and renewal (10). As such, the photoreceptor cilium experiences a very high volume of traffic, and small disruption of this transport process could potentially cause defects leading to retinal degeneration.

We have been examining the genes that when mutated cause retinal degeneration and their potential role in ciliary function in renal epithelia. We and others have demonstrated that the protein mutated in X-linked Retinitis Pigmentosa type 3 (RP3), retinitis pigmentosa GTPase regulator (RPGR), localizes to renal cilia as well as to the photoreceptor transition zone (11,12). Furthermore, RPGR directly interacts with NPHP5 and NPHP6, two proteins associated with renal–retinal diseases (13,14). In addition, we have previously shown that the Crumbs3 (Crb3) protein, which regulates apical–basal polarity also controls ciliogenesis in renal epithelia (15). Interestingly, a paralog of Crumbs3, Crumbs1, is mutated in RP12 and Leber congenital amaurosis (16).

Like *RPGR*, *RP2* is an X-linked gene that when mutated gives rise to XLRP (17–20). The *RP2* gene encodes a 350-residue polypeptide that is widely expressed. Previous work has demonstrated that RP2 is membrane associated by dual acylation of the amino-terminus, namely myristoylation at glycine 2 and palmitoylation at cysteine 3 (21). The amino-terminal half of RP2 shows both sequence and structural similarity to tubulin cofactor C (TBCC), a protein involved in the formation of alpha–beta-tubulin heterodimers. Further work has shown that this domain binds to and has GAP activity towards the small G-protein ADP ribosylation factor-like 3 (Arl3) (22). Interestingly, an Arl3 knockout mouse exhibits both cystic kidneys and retinal degeneration (23). However, the precise function of Arl3 or RP2 is unclear, although recent evidence has implicated them as potential regulators of post-Golgi traffic (24) and as a potential quality control checkpoint for cilia-destined cargo (25). In this report, we sought to identify whether RP2 may play a role in renal epithelia with specific emphasis on a potential role in primary cilia. We demonstrate that RP2 localizes to primary cilia in renal epithelia and interacts with and regulates ciliary trafficking of the product of the polycystic kidney disease 2 (*PKD2*) gene, polycystin 2. Furthermore, we present the first loss-of-function RP2 vertebrate model by morpholino-mediated knockdown of the zebrafish ortholog of RP2. Loss of function of RP2 leads to a range of developmental defects in zebrafish that are known to be associated with abnormal ciliary functions demonstrating that RP2 is essential for ciliary function during vertebrate development.

RESULTS

RP2 localizes to renal cilia

Mutations in the *RP2* gene in humans cause progressive degeneration of the photoreceptors typical of RP (17–19), yet the function of the RP2 protein is not well understood. To examine the localization and function of RP2, we generated antibodies raised against the recombinant protein that detected a single band of the predicted size in multiple cell lines (Supplementary Material, Fig. S1a and b) and first examined the localization of endogenous RP2 in the kidney (Fig. 1A). The RP2 signal was enriched in a subset of renal tubules but absent when the antibody was pre-incubated with recombinant GST-RP2 (Supplementary Material, Fig. S1c). Co-staining of kidney sections with different markers of specific nephron segments revealed that RP2 was absent from PNA (peanut agglutinin)-positive distal convoluted tubules but enriched in Tamm Horfsall-positive tubules suggesting that RP2 is expressed in the ascending loop (Fig. 1B and C, respectively). We next examined whether RP2 like other RP proteins is localized to renal cilia. Indeed immunofluorescence revealed that endogenous RP2 does localize to primary cilia in mouse kidney sections and in the MDCKII renal epithelial cell line (Figs 1D and 2A, respectively). RP2 has also been observed to localize to the base of the cilium in retinal pigmented epithelial (RPE) cells (24). When RP2 localization was examined in the ARPE19 RPE, cell line RP2 was observed to be concentrated around the base of the cilium, but absent from the cilia axoneme (Supplementary Material, Fig. S1d) as previously described (24). To confirm that ciliary localization of RP2 in renal cilia is not a staining artifact, an RP2 expression construct containing a C-terminal EGFP tag was generated. When RP2-EGFP was stably expressed in confluent MDCK cells, it localized efficiently to primary cilia (Fig. 2B). Interestingly, prior to ciliogenesis, we observed RP2-EGFP localizing predominantly around one of the centrioles (Supplementary Material, Fig. S1e). This likely corresponds to the basal body/transition zone where RP2 has been previously demonstrated to localize (26).

Localization of RP2 to cilia requires N-terminal acylation

RP2 has been previously demonstrated to be post-translationally modified at its extreme amino-terminus, specifically myristoylation at Gly2 and palmitoylation at Cys3 (27,28), and these modifications are necessary for trafficking of RP2 to the plasma membrane (28). To determine whether the membrane association of RP2 is required for ciliary targeting, a Gly2Ala (G2A) mutation was introduced into RP2-EGFP which blocks both the myristoylation and palmitoylation of RP2 (21). When G2A RP2-EGFP was introduced into MDCK cells, its cilia localization was almost completely abolished, suggesting that the membrane association of RP2 is necessary for cilia targeting (Fig. 2C). Instead, RP2-EGFP G2A was observed to accumulate in the nucleus (Fig. 2C). Introduction of a Cys3Ser (C3S) mutation in RP2 which specifically blocks palmitoylation but not myristoylation of RP2 dramatically reduced but did not abolish

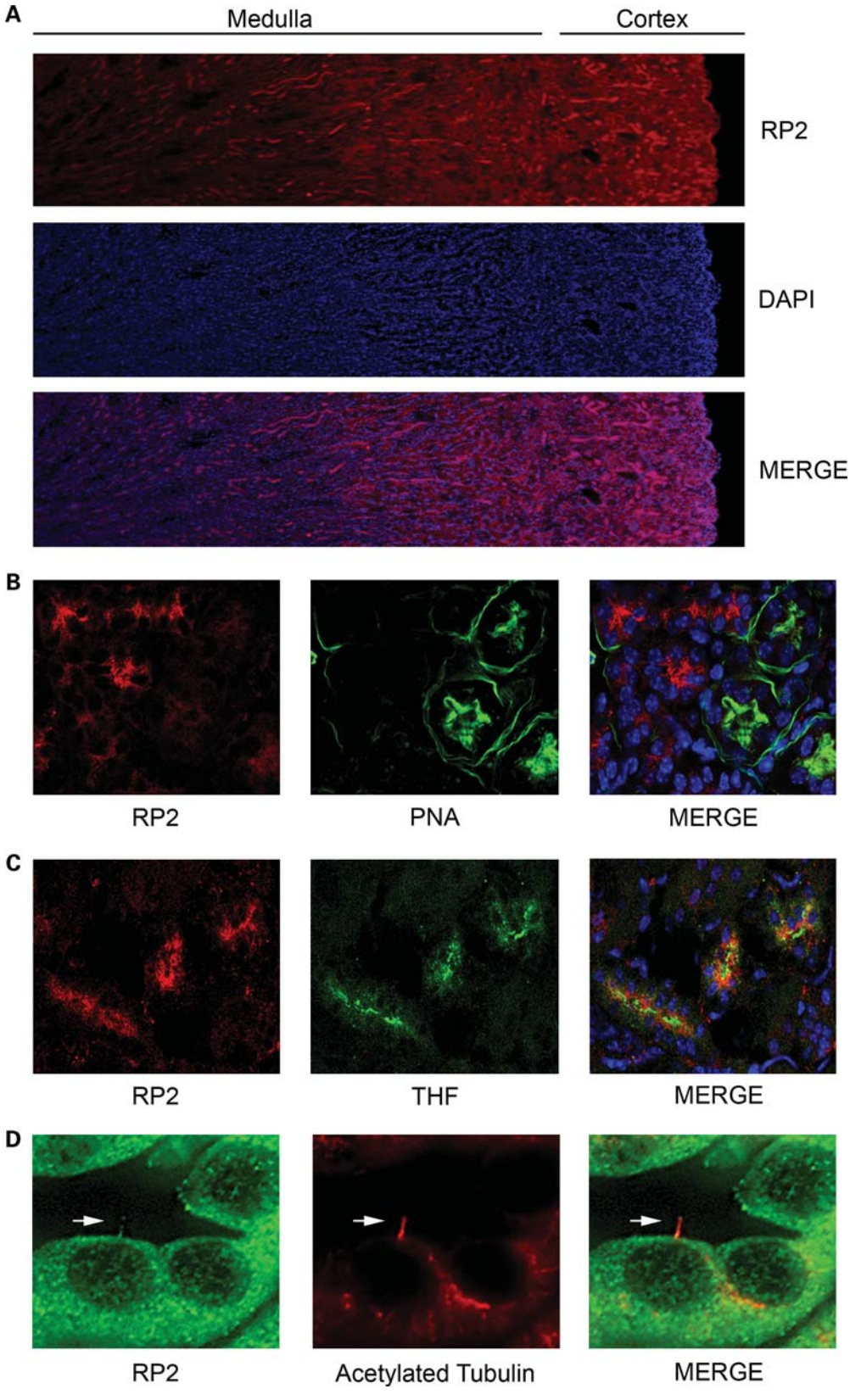

Figure 1. RP2 is enriched in distinct regions of the kidney. (**A**) RP2 staining in mouse kidney. PFA-perfused frozen mouse kidney sections were permeabilized and stained with anti-RP2 antibodies (red) and DAPI (blue) to mark nuclei. (**B**) RP2 does not localize to distal convoluted tubules. Mouse kidney sections were stained as above with the addition of peanut lectin agglutinin (PNA-FITC) to label distal convoluted tubules. (**C**) RP2 localizes to Tamm Horsfall protein (THF) positive (green) segments of the nephron. Mouse kidney sections were stained as above with the addition of anti-THF antibody. (**D**) RP2 localizes to primary cilia in mouse kidney tubules. Mouse kidney sections were stained as above with the addition of anti-acetylated tubulin to label primary cilia (red).

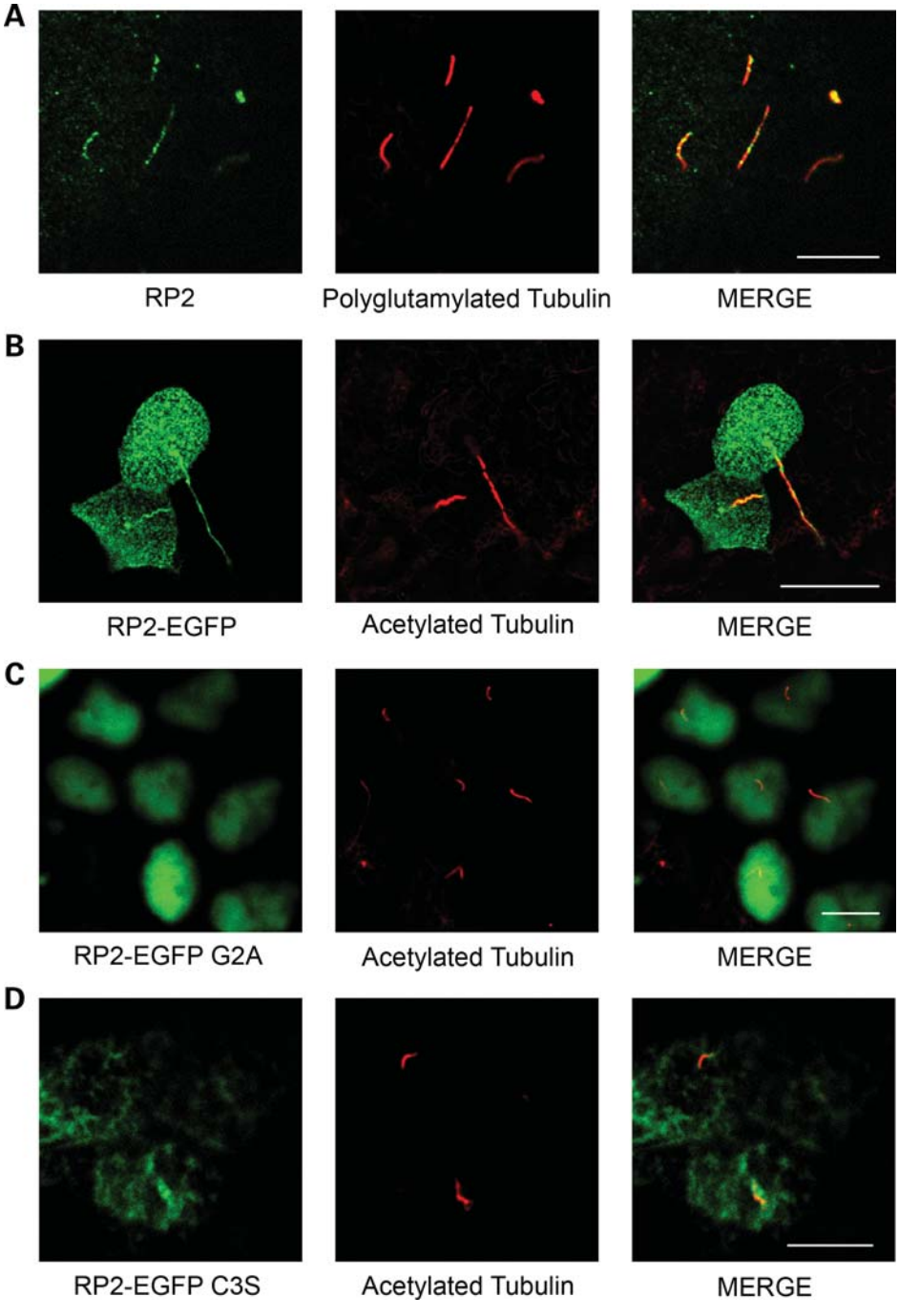

Figure 2. RP2 localizes to primary cilia. (**A**) RP2 localizes to cilia in MDCK cells. MDCK cells were grown 7 days post-confluence, fixed, permeabilized and immuno-stained using antibodies against RP2 (green) and polyglutamylated tubulin (red). (**B**) RP2-EGFP localizes to primary cilia. MDCK cells stably expressing EGFP-tagged RP2 (green) were grown for 7 days post-calcium switch to allow cilia formation. Cilia were visualized using an antibody against the cilia marker acetylated tubulin (red). (**C**) Mutation of the N-terminal myristoylation motif prevents cilia localization of RP2-EGFP and mistargets it to nuclei. MDCK cells stably expressing RP2-EGFP G2A (green) were grown for 7 days post-confluence on trans-well filters, fixed, permeabilized and immuno-stained with an anti-acetylated tubulin antibody (red). (**D**) RP2-EGFP C3S fails to target to cilia. MDCK cells stably expressing the palmitoylation mutant C3S (green) were treated as above. All scale bars (white) represent 10 μm.

ciliary localization and also did not result in nuclear accumulation (Fig. 2D).

The N-terminal TBCC-like domain of RP2 exhibits GAP activity towards the small G-protein Arl3 (22). Since it has been demonstrated that knockout of *Arl3* results in retinal degeneration and kidney cyst formation, we examined whether a pathogenic mutant of RP2 that cannot bind Arl3 (R118H) would affect trafficking of RP2 to the cilium (23). However, RP2-EGFP R118H still efficiently localized to cilia (Supplementary Material, Fig. S2a). These data suggest

that interaction of RP2 with Arl3 is not required for cilia localization of RP2.

Knockdown of RP2 by shRNA results in malformed cilia

To further explore the role of RP2 in cilia function and because loss-of-function mutations of RP2 cause retinal degeneration, we examined the effect of loss of RP2. MDCK cells were retrovirally infected with either a control shRNA against luciferase (Luc) or two different shRNAs designed against different regions of the canine RP2 transcript (RP2 shRNA nos 1 and 2) and stable pools selected. Expression of RP2 protein was efficiently ablated by both RP2 shRNA constructs (Fig. 3A). To assess the effect of RP2 knockdown on overall cell morphology and general trafficking, control and RP2 knockdown cells were seeded as single cell suspensions into Geltrex extracellular matrix. Both control and RP2 knockdown cells efficiently formed single lumen-containing cysts with a correctly polarized distribution of the lateral marker E-cadherin and the apical marker gp135 (Supplementary Material, Fig. S2b). We next asked whether RP2 is necessary for cilia formation. Control (Luc) and RP2 knockdown cells were grown on trans-well filters for 7 days post-confluence to allow cilia formation. Similar to control cells, both RP2 knockdown cell lines formed cilia as shown by staining with the cilia marker acetylated tubulin (Supplementary Material, Fig. S2c). These data suggest that RP2 is not required for cilia formation. However, when the ultra structure of cilia was examined by SEM in RP2 knockdown cells, large swellings were observed at the distal region in a large proportion of the cilia (Fig. 3B and Supplementary Material, Fig. S2d).

RP2 forms a complex with polycystin 2

Since RP2 has been implicated in the trafficking of proteins to the basal body (24), we also examined whether the observed swellings could be due to aberrant trafficking of cilia proteins. To test this hypothesis, we first examined whether any known cilia proteins could be co-immunoprecipitated with RP2 and hence enable us to examine whether mistrafficking of these proteins could be a direct cause of the observed cilia abnormalities. To efficiently immunoprecipitate RP2, MDCK cells stably expressing either empty vector (pQCXIP) or C-terminally FLAG-tagged RP2 were generated (RP2-FLAG). When RP2-FLAG was immunoprecipitated from ciliated cells, a strong co-precipitation of the endogenous cystoprotein polycystin 2 was observed (Fig. 3C). However, neither IFT88 nor Rab8 was able to co-precipitate with RP2-FLAG (data not shown). Since polycystin 2 together with polycystin 1 form a cilia-localized channel complex that raises intracellular calcium in response to cilia bending (6), we examined the effect of changes in free calcium concentration on this interaction. Addition of 5 mM calcium to the lysate greatly diminished the ability of polycystin 2 to co-immunoprecipitate with RP2 (Figs 3C and 4D). Conversely, addition of 5 mM EGTA to the lysate resulted in a stronger co-immunoprecipitation of polycystin 2 with RP2 (Fig. 3C). These results indicate that the formation of an RP2–polycystin 2 complex may be regulated by changes in intracellular calcium. We then examined whether endogenous RP2 could co-precipitate endogenous polycystin 2. Indeed, when RP2 was immunoprecipitated from bovine retinal extract, a strong co-precipitation of polycystin 2 was observed (Fig. 3E). These data confirm that these two proteins are found endogenously in a complex not only in kidney, but also in retina and perhaps other tissues.

Acylation of RP2 is required for the interaction with polycystin 2

Since we demonstrated that the membrane association of RP2 is necessary for cilia targeting, we examined the effect of the RP2 G2A mutation on the association with polycystin 2. In HEK293 cells co-transfected with wild-type polycystin 2 (PC2-V5) and the non-membrane targeting mutant of RP2 (RP2-FLAG G2A), polycystin 2 association with RP2 was almost completely abolished (Fig. 3F). These data suggest that the membrane association of RP2 is required for the interaction with polycystin 2.

It has been previously demonstrated that polycystin 2 has multiple interacting partners, and that these interactions predominantly occur through its cytoplasmic N or C-terminus (29–31). Deletion of either the N- or C-terminus of polycystin 2 (PC2-V5 ΔN and PC2-V5 ΔC, respectively) did not block the formation of an RP2–polycystin 2 complex, suggesting that neither terminus of polycystin 2 is required for interaction with RP2 (Supplementary Material, Fig. S3a and b, respectively).

RP2 regulates the ciliary mobility of polycystin 2

Since both RP2 and polycystin 2 form a complex that localizes to primary cilia, we next examined whether RP2 regulates the trafficking of polycystin 2. The localization of endogenous polycystin 2 was examined in control (Luc shRNA) and RP2 knockdown (RP2 shRNA) MDCK cells. We observed that polycystin 2 could be seen in the cilia from both cell lines, but in the RP2 knockdown cell line a marked accumulation of polycystin 2 was observed at the distal part of the cilium (Fig. 3G). To further address this, we stably expressed EGFP-tagged polycystin 2 in either control (Luc shRNA) or RP2 knockdown (RP2 shRNA) MDCK cells and examined its mobility using fluorescence recovery after photobleaching (FRAP). Intriguingly, we found that the mobility of cilium-localized polycystin 2 was greatly enhanced in RP2 knockdown cells (Fig. 4A and B). Furthermore, we also saw accumulation of EGFP-tagged polycystin 2 at the distal part of cilia in RP2 knockdown cells (Fig. 4A). We also examined the mobility of EGFP-tagged Crb3a, a single-pass transmembrane protein which we have previously demonstrated to localize to renal cilia in RP2 knockdown cells. In this case, we saw no difference in the mobility of Crb3a between control and RP2 knockdown cells (Fig. 4C). Furthermore, we also examined the localization of endogenous IFT88 in RP2 knockdown cells. In both control (Luc shRNA) and RP2 knockdown (RP2 shRNA), IFT88 was localized in a punctate manner along the length of the cilium with no apparent accumulation at the distal region of the cilium (Supplementary Material, Fig. S2e). These data suggest that RP2 may regulate ciliary

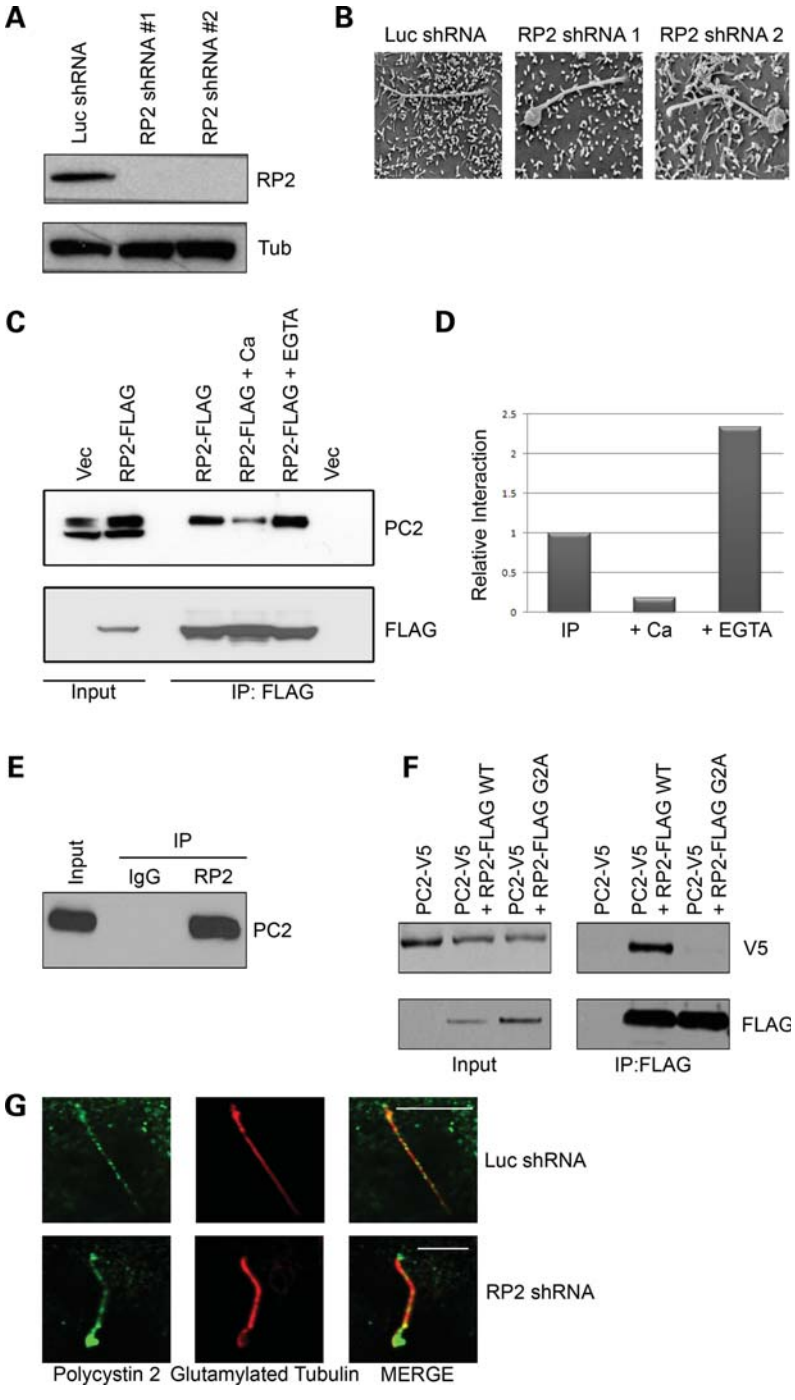

Figure 3. RP2 forms a complex with polycystin 2. (**A**) Knockdown of RP2 by retroviral shRNA. MDCK cells were retrovirally infected with either a luciferase-specific shRNA construct (Luc) or one of two separate canine-specific RP2 shRNA constructs (RP2 shRNA no. 1 and RP2 shRNA no. 2) and stable pools selected. Cell lysates were subjected to SDS–PAGE and western blotting with the indicated antibodies. (**B**) Ablation of RP2 results in swelling of the cilia tip as shown by SEM. Control or RP2 shRNA were grown 7 days post-confluence on trans-well filters, fixed and prepared for SEM imaging. (**C**) Exogenous RP2 co-immunoprecipitates endogenous polycystin 2. Cell lysates (Input) from MDCK cells stably expressing either empty vector (pQCXIP) or RP2-FLAG wild-type (WT) were subjected to anti-FLAG immunoprecipitation in the presence or absence of 5 mM calcium chloride or EGTA. Immunoprecipitates were washed and subjected to SDS–PAGE and western blotting with the antibodies indicated. (**D**) Quantification of the effect of calcium and EGTA on the co-immunoprecipitation of RP2 and polycystin 2. The western blots in (C) were subjected to densitometric analysis. (**E**) Endogenous RP2 forms a complex with endogenous polycystin 2 in retina. Lysate (Input) from bovine retina was subjected to anti-RP2 immunoprecipitation. Immunoprecipitates were washed and subjected to SDS–PAGE and western blotting with the antibodies indicated. (**F**) The membrane association of RP2 is required for the interaction with polycystin 2. HEK293 cells were transiently transfected with polycystin 2-V5 and either wild-type (WT) RP2-FLAG or the membrane targeting mutant (G2A) RP2-FLAG. Lysates were subjected to immunoprecipitation as described above. (**G**) Ablation of RP2 results in accumulation of endogenous polycystin 2 at the distal region of cilia. Control (Luc shRNA) or RP2 shRNA were grown 7 days post-confluence on trans-well filters, fixed and stained with antibodies against polycystin 2 (green) and glutamylated tubulin (red). All scale bars (white) represent 10 μm.

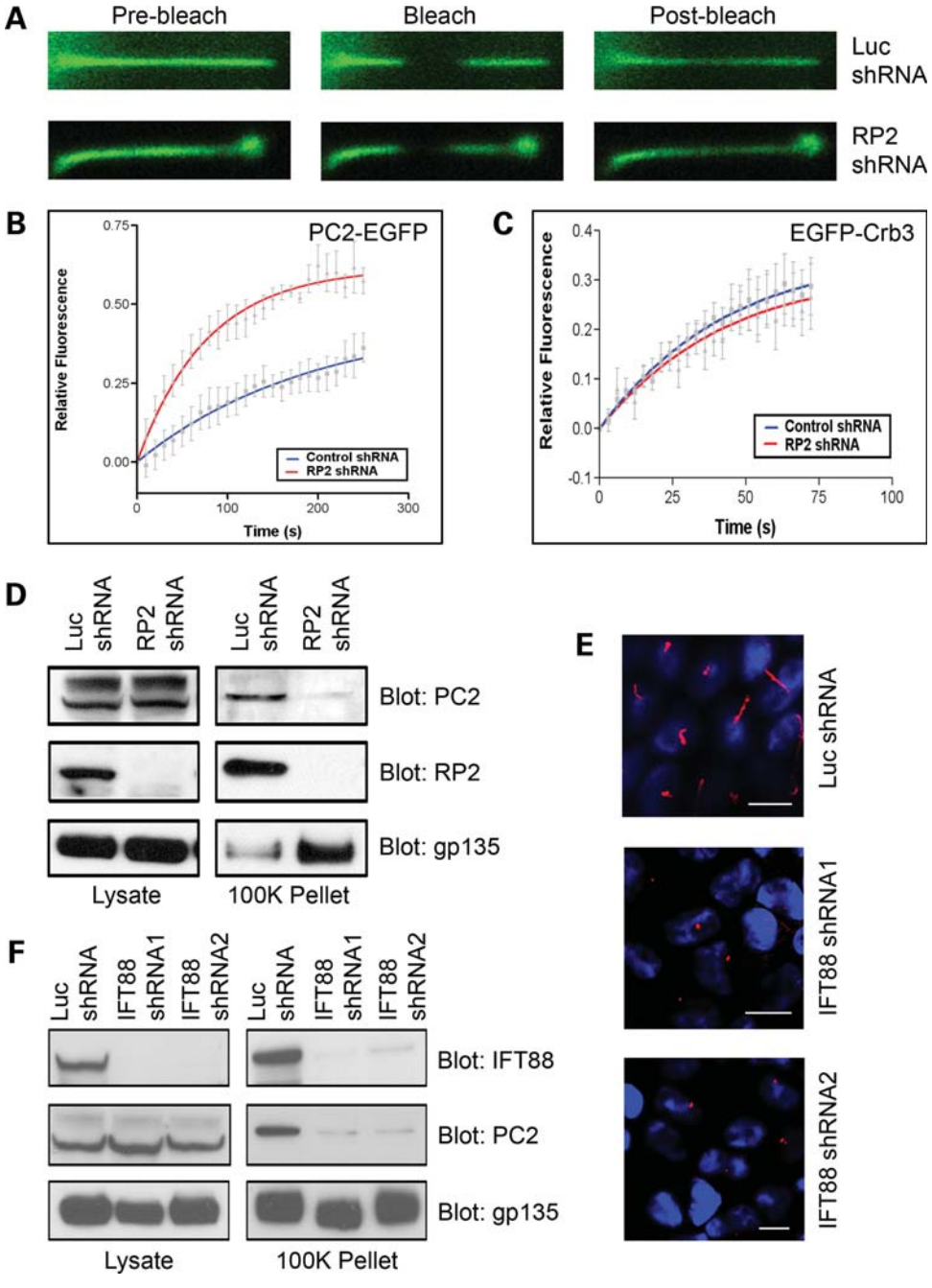

Figure 4. RP2 regulates polycystin 2 trafficking. (**A**) Ablation of RP2 results in increased mobility of cilia-localized polycystin 2. Representative FRAP confocal images from live control (Luc shRNA) or RP2 knockdown (RP2 shRNA) MDCK cells stably expressing EmGFP-tagged polycystin 2. Images show fluorescent EGFP signal pre-bleach, immediately after the bleach (Bleach) and after recovery (Post-bleach). (**B**) Average recovery after photobleach for cilia-localized polycystin2-EGFP in control (Luc shRNA, blue) and RP2 knockdown (RP2 shRNA, red). Data shown are mean ± SE, $n = 5$ cells. The solid line through the data is a single-exponential fit to the average data. (**C**) Average recovery after photobleaching for cilia-localized Crb3-EGFP in control (Luc shRNA, blue) and RP2 knockdown (RP2 shRNA, red). Data shown are mean ± SE, $n = 5$ cells. The solid line through the data is a single-exponential fit to the average data. (**D**) Ablation of RP2 results in reduced secretion of polycystin 2. Conditioned media from control (Luc shRNA) and RP2 knockdown (RP2 shRNA) cells were subjected to sequential centrifugation, and input and the 100 000*g* pellet (100K Pellet) were analyzed by western blot. (**E**) Knockdown of IFT88 results in shortened or no cilia in MDCK cells. MDCK cells were retrovirally infected with either a luciferase-specific shRNA construct (Luc) or one of two separate canine-specific IFT88 shRNA constructs (IFT88 shRNA no. 1 and IFT88 shRNA no. 2) and stable pools selected. All scale bars represent 10 μm. (**F**) Ablation of IFT88 results in reduced secretion of polycystin 2. Conditioned media from control (Luc shRNA) and IFT88 knockdown (IFT88 shRNA no. 1 and shRNA no. 2) cells were subjected to sequential centrifugation, and input and the 100 000*g* pellet (100K Pellet) were analyzed by western blot.

trafficking of a specific subset of ciliary proteins including polycystin 2.

RP2 is apically secreted

Recently polycystin 1- and polycystin 2-containing vesicles have been observed in human urine (32,33). We examined whether RP2 may be apically secreted using a differential centrifugation procedure on conditioned apical media from MDCK cells that have been used to isolate secreted vesicles (34). Interestingly, both RP2 and polycystin 2 could be seen to be enriched in the 100 000*g* pellet, indeed suggesting that these proteins are secreted (Fig. 4D—Luc shRNA). Since we have observed that polycystin 2 can be secreted from the apical side of MDCK cells, the effect of RP2 ablation on this phenomenon was examined. Conditioned media were collected from the apical side of control (Luc shRNA) and RP2 knockdown (RP2 shRNA) MDCK cells. We found that ablation of RP2 greatly reduced the amount of polycystin 2 found in the 100 000*g* pellet, suggesting that RP2 is required for the efficient secretion of polycystin 2 (Fig. 4D). However, we saw no decrease in the secretion of the non-cilia protein gp135 upon knockdown of RP2 by shRNA (Fig. 4D). These data suggest that gp135 and polycystin 2 may be secreted by different mechanisms.

Cilia are required for polycystin 2 secretion

Next we examined whether RP2 could be regulating the secretion of polycystin 2 in a cilia-dependent manner. To examine this, we ablated the expression of the key ciliogenic protein IFT88 using two different retroviral shRNA constructs targeting the canine transcript (IFT88 shRNA nos 1 and 2). Efficient knockdown of IFT88 was achieved with both constructs when compared with the control shRNA (Luc shRNA) in MDCK cells (Fig. 4F). As previously described, loss of IFT88 resulted in either very short or no cilia at all (35) in MDCK cells stably expressing the IFT88 shRNA (Fig. 4E). We examined whether polycystin 2 was secreted from the IFT88 shRNA cells which lack cilia. Conditioned media collected from the IFT88 knockdown cells revealed greatly reduced levels of secreted polycystin 2 when compared with the control cell line (Fig. 4F). However, like RP2 knockdown, knockdown of IFT88 had no effect on the secretion of the non-cilia protein gp135. These data together suggest that cilia are essential for polycystin 2 secretion.

Zebrafish RP2 traffics to cilia in mammalian cells

Since RP2 may play an important role in cilia function, we utilized a zebrafish model system to study how loss of RP2 may affect cilia-dependent developmental processes. Zebrafish have a single *rp2* gene consisting of six exons (Fig. 5A) that encode a polypeptide with high sequence homology to mammalian RP2. We first examined whether *rp2* was expressed during zebrafish embryogenesis. RT–PCR using two separate primer pairs spanning an exon–exon boundary revealed the presence of RP2 transcript from 0 h post-fertilization (hpf) through to 48 hpf (Fig. 5B). Examination of the expression pattern of RP2 by *in situ* hybridization revealed ubiquitous

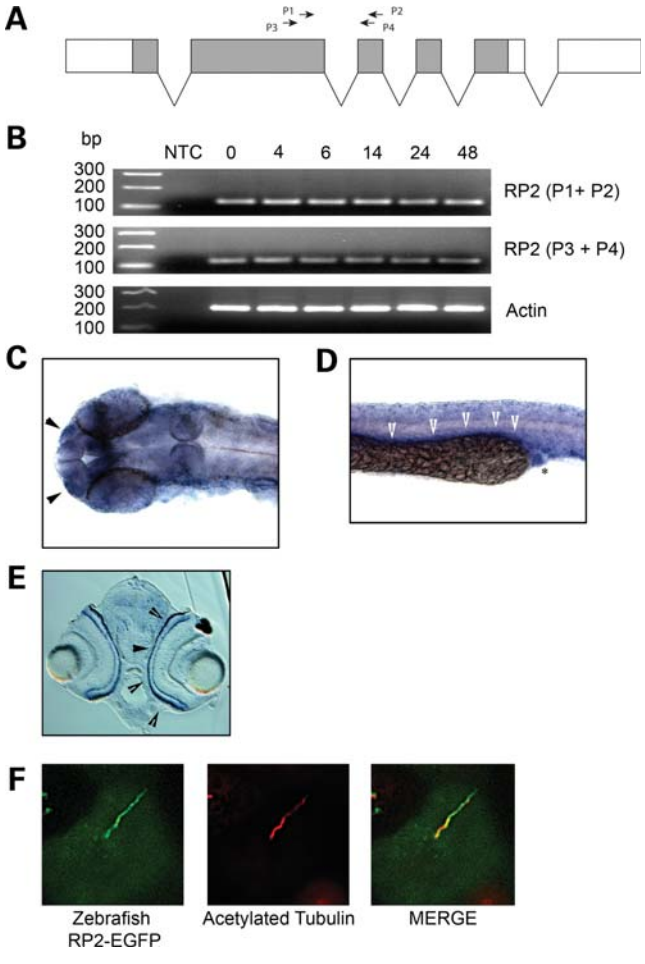

Figure 5. RP2 expression in zebrafish. (**A**) Gene structure of the Zebrafish *rp2*. Protein coding region shown in grey. Shown are the primer sets used for RT–PCR. (**B**) RT–PCR analysis of *rp2* transcript at different time points post-fertilization (hpf). NTC, no template control. (**C**) *rp2* is expressed in the olfactory placode (arrowheads). *In situ* hybridization was performed on 24 hpf embryo with an *rp2* antisense probe. (**D**) *rp2* is expressed in the pronephric duct at 24 hpf. *In situ* hybridization was performed on a 24 hpf embryo with an *rp2* antisense probe. Arrowheads show signal along the pronephric duct and asterisk shows cloaca. (**E**) *rp2* is expressed in the photoreceptor layer (arrowheads) of the retina at 72 hpf. *In situ* hybridization was performed on a 72 hpf embryo with an *rp2* antisense probe. (**F**) Zebrafish RP2 localizes to cilia in MDCK cells. MDCKII cells stably expressing zebrafish RP2-EGFP were grown for 7 days post-calcium switch to allow cilia formation. Cilia were visualized using an antibody against the cilia marker acetylated tubulin (red).

expression of the RP2 transcript throughout the embryo at 24 hpf with concentrated signals localized to the olfactory placode (Fig. 5C, arrows, and Supplementary Material, Fig. S3c) as well as in the pronephric duct (Fig. 5D, arrows, and Supplementary Material, Fig. S3d). *In situ* hybridization also revealed expression of *rp2* in the photoreceptor layer of zebrafish retina at 72 hpf (Fig. 5E), consistent with that of mammalian RP2. Since the zebrafish RP2 shows strong sequence homology to mammalian RP2 (71% sequence identity), we examined whether it may traffic in a similar manner as well. When Zebrafish RP2-EGFP was stably expressed in MDCKII cells, it also localized to the cilium (Fig. 5F). These data suggest that the Zebrafish RP2 protein may also be required for correct cilia function.

Morpholino-mediated knockdown of zebrafish RP2 results in multiple developmental defects

To investigate the role of RP2 during vertebrate development, we used morpholino-mediated knockdown of the zebrafish ortholog of RP2. A translation-blocking (AUG1) morpholino designed against the *rp2* translation initiation site effectively decreased RP2 protein levels (Fig. 6B). Following knockdown of *rp2*, zebrafish embryos exhibited a mild developmental delay (30–60 min extra to reach the 10–12 somite stage compared with mismatch control—data not shown) and multiple developmental defects that have been observed in zebrafish mutants of ciliary dysfunction, such as body curvature (Fig. 6A and Supplementary Material, Fig. S4a), hydrocephalus (Fig. 6C and D) and pericardial effusion (Fig. 6C). This phenotype could be mirrored by the use of a second translation-blocking morpholino (AUG2), although a higher dose was required (Fig. 6A). A mismatch morpholino that did not alter the protein level of *rp2* (Fig. 6B) produced no apparent phenotype (Fig. 6A). In addition, the body curvature phenotype could be partially rescued by co-injection of RNA encoding zebrafish *rp2* (Supplementary Material, Fig. S4a).

Since we have demonstrated that RP2 physically interacts with the *pkd2* gene product polycystin 2, and both mutation and loss of polycystin 2 in humans, mice and fish result in kidney cysts, we next examined whether the loss of *rp2* may also result in a cystic kidney phenotype. Indeed, knockdown of *rp2* resulted in kidney cysts in ~20% of morphants (Fig. 6E and Supplementary Material, Fig. S4b). We further explored the idea that RP2 may interact genetically with polycystin 2 by examining other defects in RP2 morphants that occur following the loss of polycystin 2. It has been previously described that the loss of polycystin 2 results in left–right patterning defects in the zebrafish embryo (36,37) and in mice (38). RP2 morphants like PKD2 morphants exhibit mislocalization of the lateral mesoderm marker southpaw (Fig. 6F and Supplementary Material, Fig. S4c), and heart looping defects in a dose-dependent manner (Figs 6G and 7A). Thus *rp2*-knockdown recapitulates the left–right asymmetry defects observed by loss of function of *pkd2* in zebrafish (36,39). Furthermore, we observed an increase in the heart looping defect upon co-injection of RP2 and PKD2 morpholinos at sub-optimal doses (Fig. 7A). These data suggest that RP2 and PKD2 function in a common developmental process.

In zebrafish, left–right asymmetry is established by the Kupffer's vesicle, a ciliated organ found transiently at the posterior of the 10–12 somite stage embryo (40). It has been previously demonstrated that correct formation and function of these cilia are necessary for the embryo to break symmetry (40). Interestingly, it has been recently demonstrated that RPGR, also an X-linked RP protein, is necessary for extension of the Kupffer's vesicle cilia in zebrafish, as *rpgr* morphants have shortened cilia compared with control morphants (41). However, upon examination of RP2 morphants, we found no observable change in the length or number of Kupffer's vesicle cilia (Fig. 7B and Supplementary Material, Fig. S4d and e). This agrees with our observation that in renal epithelia, shRNA-mediated knockdown of RP2 also does not affect ciliogenesis (Supplementary Material, Fig. S2c). Concordantly, PKD2 morphant fish also exhibit no observable defect in Kupffer's vesicle cilia formation (38). These data suggest that while RP2 may not regulate ciliogenesis, like PKD2, RP2 may be necessary for correct ciliary function.

DISCUSSION

Ciliary dysfunction is a frequent cause of severe renal cystic diseases. In this work, we have sought to identify the function of the RP2 protein with specific emphasis on its role in renal primary cilia. We have demonstrated that RP2 is enriched in the ascending loop of the kidney nephron. Furthermore, we show that RP2 localizes along the length of cilia in renal epithelial cells. This localization is in addition to the previously described localization of RP2 to apical and basolateral membrane domains (27) and to centrioles/basal bodies (24,26). Furthermore, we have demonstrated that this localization requires the acylation of the amino-terminus of RP2. This is in agreement with recent work demonstrating that acylation of RP2 is necessary for targeting of RP2 to the centrosome (24). This is highly analogous to *Cystin1*, the gene mutated in the *cpk* mouse model of polycystic kidney disease (42). Like RP2, the cystin protein localizes to cilia and is myristoylated at its amino-terminus and mutation of the cystin myristoylation site blocks its entry into the primary cilium. In addition, we demonstrate not only an interaction between RP2 and polycystin 2, but that polycystin 2 trafficking in the cilium may also be regulated by RP2. Interestingly, RP has been observed occasionally in ADPKD patients (43–46) and in a polycystin 2 mutant rat model (47), suggesting that in RP2 patients polycystin 2 dysfunction may have relevance for the disease process.

It is not clear how RP2 may regulate polycystin 2 trafficking within the cilium. The observed swellings and accumulation of polycystin 2 at the distal region of cilia are strongly indicative of a retrograde trafficking defect. However, we failed to see accumulation of IFT88 or Crb3 to this region. RP2 may be involved in specifically regulating the retrograde transport of a specific subset of ciliary cargoes such as polycystin 2. Recent work has shown that *Caenorhabditis elegans* mutants of Arl13 demonstrate abnormal cilia morphology and accumulation of PKD2 within the cilium (48). Interestingly, a very recent report has suggested that Arl13b and Arl3 may regulate IFT in a coordinated fashion (49). Since RP2 has GAP activity towards Arl3, the loss of RP2 may result in dysregulation of Arl3 and Arl13 and subsequent impairment of IFT.

Previous work has demonstrated that the loss of RP2 in retinal pigmented epithelia results in Golgi fragmentation and dispersion of IFT20 from its Golgi localization (24). However, similar to our data, the loss of RP2 expression in RPE cells does not perturb ciliogenesis. Since the loss of IFT20 results in impaired ciliogenesis, further work is required to better understand the precise mechanism by which RP2 regulates cilia trafficking and the function of IFT20 in relation to this process (50). It was previously observed that loss of RP2 results in Golgi fragmentation and defects in post-Golgi traffic in RPE cells (24). We observed that knockdown of RP2 in renal epithelial cells (MDCK) had no effect on the ability of the cells to correctly polarize and form lumen-

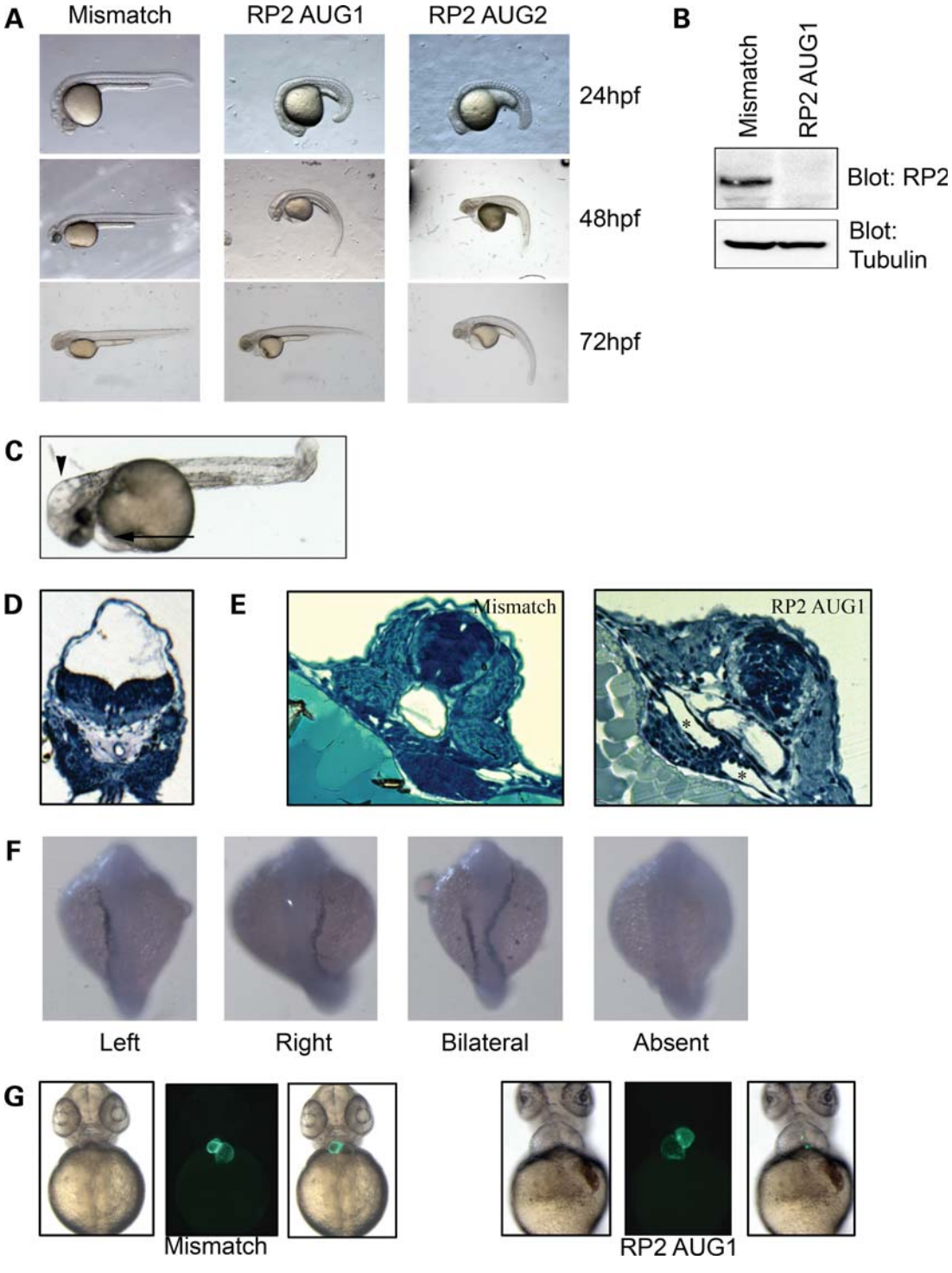

Figure 6. RP2 knockdown in zebrafish results in multiple developmental defects. (**A**) Zebrafish embryos were injected with one of two (AUG1 0.5 ng, AUG2 2 ng) translation-blocking morpholinos or a 5 bp mismatch morpholino (2 ng). (**B**) RP2 morphants have no detectable RP2 protein. Zebrafish embryos were injected with 0.5 ng of AUG1 morpholino and whole fish lysate was prepared 24 h post-injection. Lysates were subjected to SDS–PAGE and blotted with anti-RP2 antibody and alpha-tubulin as a loading control. (**C**) RP2 morphants display hydrocephalus (arrowhead) and pericardiac effusion (arrow). (**D**) Methylene blue-stained plastic-embedded section of RP2 morphants displaying prominent hydrocephalus. (**E**) RP2 morphants exhibit pronephric cysts. RP2 mismatch morphants (left panel) and RP2 AUG1 morphants were fixed at 60 hpf and plastic-embedded sections stained with methylene blue. Cysts are marked with asterisks. (**F**) RP2 morphants show left–right symmetry defects as shown by mislocalization of the lateral mesoderm marker southpaw. RP2 morphants were fixed at the 23 somite stage and *in situ* hybridization performed with an antisense southpaw probe. (**G**) RP2 morphants exhibit heart looping defects. Mismatch or RP2 AUG1 morpholinos were injected into embryos from the CMLC:EGFP zebrafish strain and heart looping was observed by fluorescence microscopy.

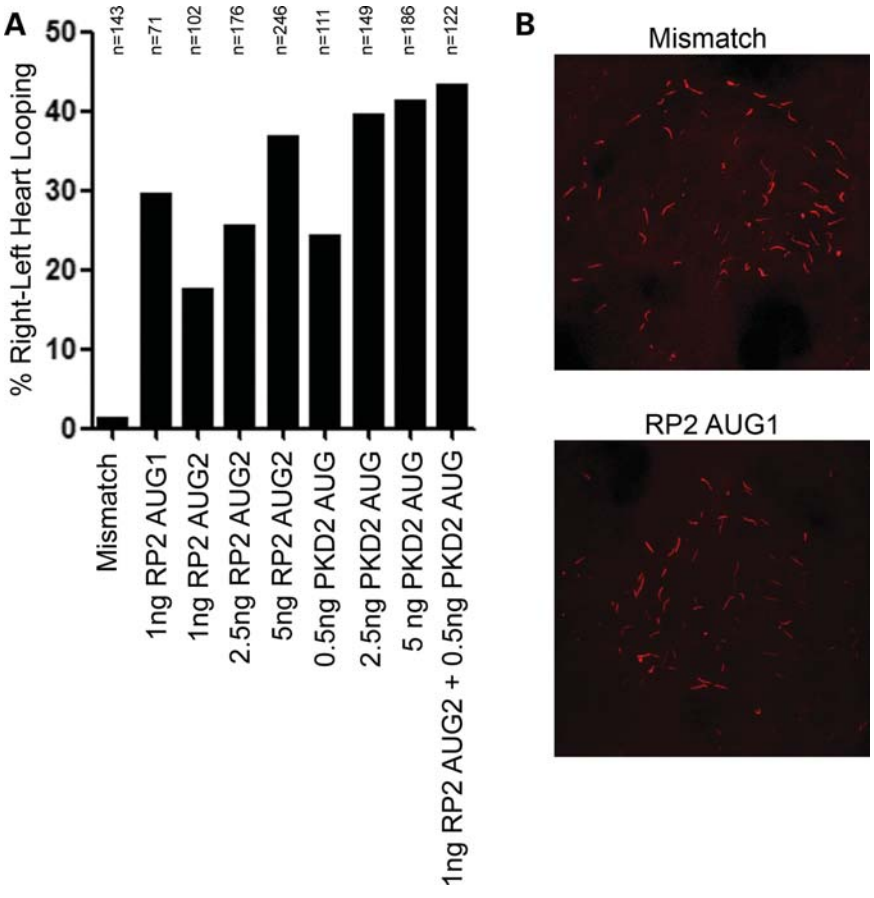

Figure 7. Combined knockdown of RP2 and PKD2 increases incorrect heart looping. (**A**) RP2 and PKD2 morpholinos were injected into CMLC:GFP zebrafish embryos at the indicated dosages. Heart looping was analyzed by fluorescence microscopy 48 hpf. (**B**) RP2 morphants have normal Kupffer's vesicle development. Zebrafish embryos were injected with either mismatch or RP2 morpholinos. Embryos were fixed at the 10–12 somite stage and stained for acetylated tubulin (red).

containing cysts. Since cell polarity is dependent on correct intracellular trafficking, more study is necessary to determine the exact pathways in the Golgi that are impacted by RP2.

We have demonstrated that both RP2 and polycystin 2 are secreted from the apical side of MDCK cells. In addition, it appears that this process is regulated by RP2 as depletion of RP2 results in reduction in polycystin 2 secretion. This process appears to be cilia dependent as inhibition of cilia formation by IFT88 knockdown results in reduced polycystin 2 secretion. However, IFT88 may be regulating this process at the level of exocytosis as it has been recently demonstrated that IFT proteins, namely IFT20, are also required for membrane trafficking (51,52). Of particular interest was our observation that knockdown of RP2 leads to swelling of distal tips of cilia that phenotypically resemble those seen in BBS knockout and aln mutant mice (53,54). Since polycystin 2 was observed to accumulate in malformed cilia following knockdown of RP2, we hypothesize that RP2 can potentially regulate cilia-dependent polycystin 2 secretion. Interestingly, vesicle budding has been observed from the tips of *Chlamydomonas* flagella (51). Consideration of the structure and function of the photoreceptor outer segment (a modified cilium) suggests this secretion may be a function common to certain cilia. Photoreceptor outer segments contain numerous rhodopsin-containing membranous discs that mediate light-induced signaling. At the distal portion of the outer segment, these discs are shed and subsequently engulfed by the overlying retinal pigmented epithelium. Perturbations in outer segment disc shedding are associated with severe retinal degenerative diseases (10). Hence, if RP2 is intrinsically involved in cilia-based secretion, the loss or mutation of RP2 could adversely affect the shedding of membrane discs from the distal end of the photoreceptor outer segment leading to retinal degeneration. Further studies are being carried out to understand this process.

To date, no extra-retinal phenotype has been reported in *RP2* patients. Due to the low frequency of RP2 mutations (5–10% of all XLRP cases), we surmise that these may have been overlooked. Our study suggests that the loss of RP2 function in humans may result in a more severe and syndromic phenotype or lethality. It is, therefore, possible that RP2 mutations reported so far may not be complete null and perhaps retain partial function (hypomorphic alleles). Given the high trafficking demands of photoreceptors, subtle changes in RP2 function due to hypomorphic mutations may result in deleterious effects in photoreceptors while sparing other tissues. Our genetic interactions further suggest that hypomorphic RP2 mutations may act as modifiers of kidney

phenotype in NPHP or PKD patients. Moreover, recent reports demonstrated that silencing of the other XLRP protein RPGR can also result in developmental disorders and renal cysts (41,55). These phenotypes have not been reported in XLRP patients thus far. However, combined knockdown of rpgr and its interacting cystic protein NPHP6 results in increased observation of renal cysts. This and other reports in conjunction with our data highlight the growing phenomenon of both genetic and physical interactions between ciliopathy proteins. Further work is being undertaken to examine how RP2 function may intercede with other known ciliopathy pathways.

MATERIALS AND METHODS

Antibodies

Rabbit anti-RP2 antibody was generated by immunizing rabbits with full-length recombinant human GST-RP2 (Cocalico Biologicals Inc., Reamstown, PA, USA). Affinity purified antibody was purified using immobilized recombinant HIS-RP2. Affinity purified antibody was tested for its ability to detect overexpressed RP2-FLAG. Mouse anti-acetylated tubulin, anti-gamma tubulin, anti-polyglutamylated tubulin, anti-FLAG, anti-rhodopsin, rabbit anti-actin, anti-Kif17, anti-Kif3a and rat anti-E-cadherin were obtained from Sigma (Sigma Aldrich, St Louis, MO, USA). Mouse anti-Rab8 was obtained from BD Biosciences (San Jose, CA, USA). Rabbit anti-V5 was obtained from Bethyl Labs (Bethyl Laboratories Inc., Montgomery, TX, USA). Rabbit anti-IFT20 was obtained from Proteintech (Proteintech Group Inc., Chicago, IL, USA). Rabbit anti-ninein was obtained from BioLegend (San Diego, CA, USA). Wheat-germ agglutinin Alexa594 was obtained from Invitrogen (Carlsbad, CA, USA). Rabbit anti-polycystin 2 (YCC2) and rabbit anti-IFT88 were kindly provided by Stefan Somlo (Yale University) and Bradley Yoder (University of Alabama at Birmingham), respectively. Rabbit anti-Crb3 was as previously described (15).

Cell culture

HEK293 and MDCKII cells were grown in DMEM and ARPE-19 cells were grown in DMEM:F12, supplemented with 10% FBS, 100 units of penicillin, 100 μg/ml streptomycin sulfate and 2 mM L-glutamine. For cyst assays, control or RP2 shRNA cells were trypsinized for 30 min, resuspended in DMEM with 2% Geltrex (Invitrogen) and seeded on a 100% Geltrex base in 8-well chamber coverslips (Labtek, Nunc, Rochester, NY, USA) using 250 μl of 2×10^4 cells/ml for each well.

Constructs

To generate RP2-EGFP, full-length human RP2 was amplified by PCR from a full-length EST (cDNA clone 5520795, Open Biosystems, Huntsville, AL, USA) and subcloned into pEGFP-N1 (Clontech, Mountain View, CA, USA). To generate RP2-FLAG, full-length human RP2 was amplified by PCR incorporating the coding sequence for the FLAG epitope into the 3′ PCR primer. The PCR product was then inserted into the retroviral vector pQCXIP (Clontech). For shRNA, oligos were annealed and ligated into pSIREN-RetroQ as per the manufacturer's instructions (Clontech). shRNA targets were as follows: RP2 shRNA no. 1—GGAGCAACATTCATGACT TTA, RP2 shRNA no. 2—GCAGTGATGAATCATGCTTAG, IFT88 shRNA no. 1—GGATATGGGTCCAAGACATCC, IFT88 shRNA no. 2—GCACTAGATCAAATTCCAAGT. For polycystin 2 constructs, mouse polycystin 2 was amplified by PCR and inserted into the pENTR-DTOPO gateway vector (Invitrogen). For generation of V5 or EmGFP-tagged polycystin 2, the polycystin 2 orf was recombined into pCDNA-DEST40 or pCDNA6.2-C-EmGFP-DEST, respectively (Invitrogen). EGFP-Crb3 was cloned into pREVTRE (Clontech).

Generation of stable MDCK cell lines

HEK293T cells were transiently transfected with pGAG/POL and pVSVG plus either pQCXIP for stable protein expression or pSIREN-RetroQ for shRNA expression (Clontech). Virus-containing media was collected, filtered though a 0.4 μm filter and mixed with an equal volume of fresh culture media. Polybrene (Clontech) was added to 4 μg/ml and virus was added to MDCKII cells. Twelve hours later, media were replaced. Forty-eight hours post-infection, stable expressing pools were selected using media containing 5 μg/ml Puromycin (Invitrogen). For RP2-EGFP stable cell lines, MDCKII cells were stably transfected using Fugene 6 reagent (Roche Diagnostics, Indianapolis, IN, USA) under 600 μg/ml G418 selection (Invitrogen). For generation of polycystin 2-EmGFP and EGFP-Crb3 stable MDCK cells, either Luc shRNA or RP2 shRNA stable cells were stably transfected with polycystin 2-EmGFP or EGFP-Crb3 as previously described and stable pools selected using media containing 10 μg/ml Blasticidin (Invitrogen) or 200 μg/ml Hygromycin B (Roche), respectively.

Immunofluorescence

Cell lines were grown for 7 days post-confluence on trans-well filters (Corning). Cells were then fixed in 4% paraformaldehyde/PBS, permeabilized with 0.1% TX100/PBS and blocked with 2% goat serum/PBS. For gamma-tubulin staining, cells were fixed and permeabilized in ice-cold acetone/methanol prior to blocking. Primary antibodies were incubated with samples in 2% goat serum/PBS overnight at 30°C. Alexafluorophore-conjugated secondary antibodies (Invitrogen) were incubated with samples in blocking buffer for 1 h at 30°C. Samples were mounted using ProLong Gold antifade reagent (Invitrogen). Mouse retinal sections were purchased from the University of Michigan Center for Organogenesis Morphology Core. Immuno-EM was performed as previously described (56).

Immunoprecipitation and western blotting

Immunoprecipitation and western blotting were performed as previously described (57). All inputs shown are 5% of material used for immunoprecipitations. Densitometry was performed using Quantity One software (BioRad).

Preparation of conditioned media

MDCK cells were seeded onto trans-well filters and grown for 7 days post-confluence. After 7 days, the apical chamber was washed twice with serum-free medium and serum-free medium applied. Cells were grown for a further 48 h after which time the apical medium was removed and placed on ice and protease inhibitor cocktail added (Sigma). The medium was then subjected to centrifugation at 500*g* for 10 min, 2000*g* for 10 min, 10 000*g* for 30 min and 100 000*g* for 90 min. Pellets from each step were solubilized in sample buffer and subjected to SDS–PAGE.

Fish breeding and maintenance

Zebrafish (*Danio rerio*) were reared and maintained as previously described (ref. Zebrafish book). Embryos were collected after natural spawns, kept at 28.5°C and staged according to hpf. A laboratory inbred AB* wild-type strain was used.

RT–PCR and cDNA cloning

A BLAST search for zebrafish *rp2* gene was performed using the protein sequence of human RP2 (Genbank accession NP_008846). The zebrafish genome database (http://www.ensembl.org/Danio_rerio/) was searched for genomic sequences and the acquired genomic sequences were analyzed with Genscan software (http://genes.mit.edu/GENSCAN.html) to determine the potential coding exons. Based on the sequence analysis results, primers were designed for RT–PCR. Total RNA was isolated from 60 hpf embryos using Tri-reagent (Invitrogen) and reverse-transcribed with oligo-dT primers and Superscript II reverse transcriptase (Invitrogen) following the manufacturer's protocol (Superscript II manual, version 11-11-203). RT–PCR was carried out following standard protocol and the PCR products were gel-purified, cloned into the Promega T-easy vector (Promega, Madison, WI, USA) and sequenced at the University of Michigan Sequencing Core. Sequence alignment (Clustal W method) was done with the Lasergene software (DNAStar, Madison, WI, USA). Primers for cloning the cDNA of zebrafish *rp2* for *in situ* probe construction were: 5′-CCAGGGTCAAGG AAACGG (forward); 5′-ACGATTAATGCTCCTGTTTAGT AGTACA (reverse). Primers for the rp2 orf expression construct were 5′-ATGGGGTGCTTCTTCTCCAAAAAATCGA GGAGG (forward); 5′-TCACAGGCCCATCTGCAT (reverse). Primers for RT–PCR were: set 1, 5′-GAGACTACACCACTG CTAATG (forward) and ATTATTCTGGAACACTCGGCT (reverse); set 2, 5′-GAGTCTTGTCTGTTTGTGTT (forward) and ATGGAAACCTCTTTAGTCTGA (reverse).

In situ hybridization

In situ hybridization was carried out as previously described (58). To prevent pigmentation for expression analysis after 24 hpf, embryos were transferred to water containing 0.2 mM 1-phenyl-2-thiourea at 20 hpf and fixed at appropriate stages. The DIG-labeled probes for zebrafish rp2 were *in vitro* synthesized from the cloned cDNA. The probe for southpaw is a gift from Dr R.D. Burdine (36).

Morpholino oligo-mediated knockdown

To knock down zebrafish RP2, two morpholino oligos were synthesized (Gene-Tools). The translation-blocking morpholino oligos (AUG1-MO) (5′-tttggagaagaagcaccccatttat) and (AUG2-MO) (5′-TGCTATTTGTCAGCACGCCCCTCCG) were used. The PKD2 AUG used was as previously described (36). The 5-base mismatch morpholino oligo (5′-tttcgacaacaa ggacccgatttat) was used as negative control. The MOs were dissolved in nuclease-free water and injected into zebrafish embryos at 1–4-cell stages in 0.1 M KCl at the specified dosage. The injection volume is estimated to be 1–2 nl. To rescue the MO-induced phenotype, the zebrafish *rp2* gene was cloned into pcDNA-6.2-EmGFP vector. Conservative mutations were introduced into the AUG1-MO target region. Capped RNA was *in vitro* synthesized with mMessenger mMachine T7 kit (Ambion). Approximately 100 ng of RNA was co-injected with MOs.

Histology

Zebrafish embryos were fixed with 4% PFA overnight, serial-dehydrated with 25, 50, 75 and 95% ethanol and then equilibrated with JB-4 solution (Polysciences) overnight at 4°C. The embryos were embedded in JB-4 resin and sectioned with a Leica R2265 microtome. The sections were stained with methylene blue as previously described (58).

Immunohistochemistry

Zebrafish embryos were fixed with Dent's fixative (80% methanol, 20% DMSO), rehydrated with 1× PBS and blocked at room temperature for 2 h with the incubation buffer (2 mg/ml BSA, 1% DMSO, 0.2% Triton X-100, 1× PBS pH 7.4) containing 10% serum. After blocking, the embryos were incubated with anti-acetylated tubulin antibody (1:500; Sigma) and Alex594-conjugated anti-mouse IgG (1:1000) (Invitrogen), respectively, at 4°C overnight. The confocal images were captured with a Leica SP5X laser scanning microscope and analyzed with LAS AF software (Leica).

SUPPLEMENTARY MATERIAL

Supplementary Material is available at *HMG* online.

ACKNOWLEDGEMENTS

The electron microscopy studies were performed at the Indiana University School of Medicine EM Center; thanks to the generous support of that facility by the Polycystic Kidney Disease Foundation. We acknowledge Dr Sam Straight of the CLCI for his help in data acquisition and analysis. F.H. is an Investigator of the Howard Hughes Medical Institute, a Doris Duke Distinguished Clinical Scientist and a Frederick G. L. Huetwell Professor.

Conflict of Interest statement. None declared.

FUNDING

This work was supported by grants from the PKD foundation (B.M.—162G08a), NIH (J.M.—DC009606; P.J.—DC009524; F.H.—DK1069274, DK1068306, DK064614; B.M.—DK084725), NEI (H.K.—EY007961 and intramural funds to A.S.) and The Foundation Fighting Blindness (H.K.). T.H. was supported by a fellowship from the PKD Foundation (92a2f).

REFERENCES

1. Qin, H., Diener, D.R., Geimer, S., Cole, D.G. and Rosenbaum, J.L. (2004) Intraflagellar transport (IFT) cargo: IFT transports flagellar precursors to the tip and turnover products to the cell body. *J. Cell Biol.*, **164**, 255–266.
2. Rosenbaum, J. (2002) Intraflagellar transport. *Curr. Biol.*, **12**, R125.
3. Cole, D.G., Diener, D.R., Himelblau, A.L., Beech, P.L., Fuster, J.C. and Rosenbaum, J.L. (1998) Chlamydomonas kinesin-II-dependent intraflagellar transport (IFT): IFT particles contain proteins required for ciliary assembly in *Caenorhabditis elegans* sensory neurons. *J. Cell Biol.*, **141**, 993–1008.
4. Katsanis, N. (2004) The oligogenic properties of Bardet–Biedl syndrome. *Hum. Mol. Genet.*, **13** (Review Issue 1), R65–R71.
5. Pretorius, D.H. and Reznik, V. (2007) Senior-Loken syndrome. *J. Ultrasound Med.*, **26**, 418.
6. Nauli, S.M., Alenghat, F.J., Luo, Y., Williams, E., Vassilev, P., Li, X., Elia, A.E., Lu, W., Brown, E.M., Quinn, S.J. *et al.* (2003) Polycystins 1 and 2 mediate mechanosensation in the primary cilium of kidney cells. *Nat. Genet.*, **33**, 129–137.
7. Jones, C., Roper, V.C., Foucher, I., Qian, D., Banizs, B., Petit, C., Yoder, B.K. and Chen, P. (2008) Ciliary proteins link basal body polarization to planar cell polarity regulation. *Nat. Genet.*, **40**, 69–77.
8. Fischer, E., Legue, E., Doyen, A., Nato, F., Nicolas, J.F., Torres, V., Yaniv, M. and Pontoglio, M. (2006) Defective planar cell polarity in polycystic kidney disease. *Nat. Genet.*, **38**, 21–23.
9. Rosenbaum, J.L., Cole, D.G. and Diener, D.R. (1999) Intraflagellar transport: the eyes have it. *J. Cell Biol.*, **144**, 385–388.
10. Young, R.W. (1974) Proceedings: biogenesis and renewal of visual cell outer segment membranes. *Exp. Eye Res.*, **18**, 215–223.
11. Khanna, H., Hurd, T.W., Lillo, C., Shu, X., Parapuram, S.K., He, S., Akimoto, M., Wright, A.F., Margolis, B., Williams, D.S. *et al.* (2005) RPGR-ORF15, which is mutated in retinitis pigmentosa, associates with SMC1, SMC3, and microtubule transport proteins. *J. Biol. Chem.*, **280**, 33580–33587.
12. Hong, D.H., Pawlyk, B., Sokolov, M., Strissel, K.J., Yang, J., Tulloch, B., Wright, A.F., Arshavsky, V.Y. and Li, T. (2003) RPGR isoforms in photoreceptor connecting cilia and the transitional zone of motile cilia. *Invest. Ophthalmol. Vis. Sci.*, **44**, 2413–2421.
13. Chang, B., Khanna, H., Hawes, N., Jimeno, D., He, S., Lillo, C., Parapuram, S.K., Cheng, H., Scott, A., Hurd, R.E. *et al.* (2006) In-frame deletion in a novel centrosomal/ciliary protein CEP290/NPHP6 perturbs its interaction with RPGR and results in early-onset retinal degeneration in the rd16 mouse. *Hum. Mol. Genet.*, **15**, 1847–1857.
14. Otto, E.A., Loeys, B., Khanna, H., Hellemans, J., Sudbrak, R., Fan, S., Muerb, U., O'Toole, J.F., Helou, J., Attanasio, M. *et al.* (2005) Nephrocystin-5, a ciliary IQ domain protein, is mutated in Senior-Loken syndrome and interacts with RPGR and calmodulin. *Nat. Genet.*, **37**, 282–288.
15. Fan, S., Hurd, T.W., Liu, C.J., Straight, S.W., Weimbs, T., Hurd, E.A., Domino, S.E. and Margolis, B. (2004) Polarity proteins control ciliogenesis via kinesin motor interactions. *Curr. Biol.*, **14**, 1451–1461.
16. Richard, M., Roepman, R., Aartsen, W.M., van Rossum, A.G., den Hollander, A.I., Knust, E., Wijnholds, J. and Cremers, F.P. (2006) Towards understanding CRUMBS function in retinal dystrophies. *Hum. Mol. Genet.*, **15** (Review Issue 2), R235–R243.
17. Schwahn, U., Lenzner, S., Dong, J., Feil, S., Hinzmann, B., van Duijnhoven, G., Kirschner, R., Hemberger, M., Bergen, A.A., Rosenberg, T. *et al.* (1998) Positional cloning of the gene for X-linked retinitis pigmentosa 2. *Nat. Genet.*, **19**, 327–332.
18. Hardcastle, A.J., Thiselton, D.L., Van Maldergem, L., Saha, B.K., Jay, M., Plant, C., Taylor, R., Bird, A.C. and Bhattacharya, S. (1999) Mutations in the RP2 gene cause disease in 10% of families with familial X-linked retinitis pigmentosa assessed in this study. *Am. J. Hum. Genet.*, **64**, 1210–1215.
19. Breuer, D.K., Yashar, B.M., Filippova, E., Hiriyanna, S., Lyons, R.H., Mears, A.J., Asaye, B., Acar, C., Vervoort, R., Wright, A.F. *et al.* (2002) A comprehensive mutation analysis of RP2 and RPGR in a North American cohort of families with X-linked retinitis pigmentosa. *Am. J. Hum. Genet.*, **70**, 1545–1554.
20. Mears, A.J., Gieser, L., Yan, D., Chen, C., Fahrner, S., Hiriyanna, S., Fujita, R., Jacobson, S.G., Sieving, P.A. and Swaroop, A. (1999) Protein-truncation mutations in the RP2 gene in a North American cohort of families with X-linked retinitis pigmentosa. *Am. J. Hum. Genet.*, **64**, 897–900.
21. Chapple, J.P., Grayson, C., Hardcastle, A.J., Bailey, T.A., Matter, K., Adamson, P., Graham, C.H., Willison, K.R. and Cheetham, M.E. (2003) Organization on the plasma membrane of the retinitis pigmentosa protein RP2: investigation of association with detergent-resistant membranes and polarized sorting. *Biochem. J.*, **372**, 427–433.
22. Veltel, S., Gasper, R., Eisenacher, E. and Wittinghofer, A. (2008) The retinitis pigmentosa 2 gene product is a GTPase-activating protein for Arf-like 3. *Nat. Struct. Mol. Biol.*, **15**, 373–380.
23. Schrick, J.J., Vogel, P., Abuin, A., Hampton, B. and Rice, D.S. (2006) ADP-ribosylation factor-like 3 is involved in kidney and photoreceptor development. *Am. J. Pathol.*, **168**, 1288–1298.
24. Evans, R.J., Schwarz, N., Nagel-Wolfrum, K., Wolfrum, U., Hardcastle, A.J. and Cheetham, M.E. (2010) The retinitis pigmentosa protein RP2 links pericentriolar vesicle transport between the Golgi and the primary cilium. *Hum. Mol. Genet.*, **19**, 1358–1367.
25. Stephan, A., Vaughan, S., Shaw, M.K., Gull, K. and McKean, P.G. (2007) An essential quality control mechanism at the eukaryotic basal body prior to intraflagellar transport. *Traffic*, **8**, 1323–1330.
26. Blacque, O.E., Perens, E.A., Boroevich, K.A., Inglis, P.N., Li, C., Warner, A., Khattra, J., Holt, R.A., Ou, G., Mah, A.K. *et al.* (2005) Functional genomics of the cilium, a sensory organelle. *Curr. Biol.*, **15**, 935–941.
27. Chapple, J.P., Hardcastle, A.J., Grayson, C., Spackman, L.A., Willison, K.R. and Cheetham, M.E. (2000) Mutations in the N-terminus of the X-linked retinitis pigmentosa protein RP2 interfere with the normal targeting of the protein to the plasma membrane. *Hum. Mol. Genet.*, **9**, 1919–1926.
28. Chapple, J.P., Hardcastle, A.J., Grayson, C., Willison, K.R. and Cheetham, M.E. (2002) Delineation of the plasma membrane targeting domain of the X-linked retinitis pigmentosa protein RP2. *Invest. Ophthalmol. Vis. Sci.*, **43**, 2015–2020.
29. Tsiokas, L., Kim, E., Arnould, T., Sukhatme, V.P. and Walz, G. (1997) Homo- and heterodimeric interactions between the gene products of PKD1 and PKD2. *Proc. Natl Acad. Sci. USA*, **94**, 6965–6970.
30. Rundle, D.R., Gorbsky, G. and Tsiokas, L. (2004) PKD2 interacts and co-localizes with mDia1 to mitotic spindles of dividing cells: role of mDia1 in PKD2 localization to mitotic spindles. *J. Biol. Chem.*, **279**, 29728–29739.
31. Li, X., Luo, Y., Starremans, P.G., McNamara, C.A., Pei, Y. and Zhou, J. (2005) Polycystin-1 and polycystin-2 regulate the cell cycle through the helix-loop-helix inhibitor Id2. *Nat. Cell Biol.*, **7**, 1202–1212.
32. Pisitkun, T., Shen, R.F. and Knepper, M.A. (2004) Identification and proteomic profiling of exosomes in human urine. *Proc. Natl Acad. Sci. USA*, **101**, 13368–13373.
33. Hogan, M.C., Manganelli, L., Woollard, J.R., Masyuk, A.I., Masyuk, T.V., Tammachote, R., Huang, B.Q., Leontovich, A.A., Beito, T.G., Madden, B.J. *et al.* (2009) Characterization of PKD protein-positive exosome-like vesicles. *J. Am. Soc. Nephrol.*, **20**, 278–288.
34. Raposo, G., Nijman, H.W., Stoorvogel, W., Liejendekker, R., Harding, C.V., Melief, C.J. and Geuze, H.J. (1996) B lymphocytes secrete antigen-presenting vesicles. *J. Exp. Med.*, **183**, 1161–1172.
35. Pazour, G.J., Dickert, B.L., Vucica, Y., Seeley, E.S., Rosenbaum, J.L., Witman, G.B. and Cole, D.G. (2000) Chlamydomonas IFT88 and its mouse homologue, polycystic kidney disease gene tg737, are required for assembly of cilia and flagella. *J. Cell Biol.*, **151**, 709–718.

36. Schottenfeld, J., Sullivan-Brown, J. and Burdine, R.D. (2007) Zebrafish curly up encodes a Pkd2 ortholog that restricts left-side-specific expression of southpaw. *Development*, **134**, 1605–1615.
37. Pennekamp, P., Karcher, C., Fischer, A., Schweickert, A., Skryabin, B., Horst, J., Blum, M. and Dworniczak, B. (2002) The ion channel polycystin-2 is required for left–right axis determination in mice. *Curr. Biol.*, **12**, 938–943.
38. Bisgrove, B.W., Snarr, B.S., Emrazian, A. and Yost, H.J. (2005) Polaris and Polycystin-2 in dorsal forerunner cells and Kupffer's vesicle are required for specification of the zebrafish left–right axis. *Dev. Biol.*, **287**, 274–288.
39. Obara, T., Mangos, S., Liu, Y., Zhao, J., Wiessner, S., Kramer-Zucker, A.G., Olale, F., Schier, A.F. and Drummond, I.A. (2006) Polycystin-2 immunolocalization and function in zebrafish. *J. Am. Soc. Nephrol.*, **17**, 2706–2718.
40. Essner, J.J., Amack, J.D., Nyholm, M.K., Harris, E.B. and Yost, H.J. (2005) Kupffer's vesicle is a ciliated organ of asymmetry in the zebrafish embryo that initiates left–right development of the brain, heart and gut. *Development*, **132**, 1247–1260.
41. Ghosh, A.K., Murga-Zamalloa, C.A., Chan, L., Hitchcock, P.F., Swaroop, A. and Khanna, H. (2010) Human retinopathy-associated ciliary protein retinitis pigmentosa GTPase regulator mediates cilia-dependent vertebrate development. *Hum. Mol. Genet.*, **19**, 90–98.
42. Tao, B., Bu, S., Yang, Z., Siroky, B., Kappes, J.C., Kispert, A. and Guay-Woodford, L.M. (2009) Cystin localizes to primary cilia via membrane microdomains and a targeting motif. *J. Am. Soc. Nephrol.*, **20**, 2570–2580.
43. Mavromatidis, K., Sombolos, K., Zoumbaridis, N., Natse, T., Panidou-Kiriakidou, I. and Hagekostas, G. (1992) Retinitis pigmentosa and aortic regurgitation in a patient with adult polycystic kidney disease. *Nephron*, **60**, 114–115.
44. Kocyigit, I., Unal, A., Ozaslan, E., Oymak, O. and Utas, C. (2010) Does retinitis pigmentosa relate with polycystic kidney disease? *Int. Urol. Nephrol*., in press.
45. Perng, C.T. and Segasothy, M. (2008) Retinitis pigmentosa associated with autosomal dominant polycystic kidney disease. *Nephrology*, **4**, 37–39.
46. Narendran, N., Guymer, R.H., Cain, M. and Baird, P.N. (2004) Identification of a mutation in the PKD2 gene in a family with age-related macular degeneration. *Am. J. Med. Genet. A*, **127A**, 208–210.
47. Gallagher, A.R., Hoffmann, S., Brown, N., Cedzich, A., Meruvu, S., Podlich, D., Feng, Y., Konecke, V., de Vries, U., Hammes, H.P. *et al.* (2006) A truncated polycystin-2 protein causes polycystic kidney disease and retinal degeneration in transgenic rats. *J. Am. Soc. Nephrol.*, **17**, 2719–2730.
48. Cevik, S., Hori, Y., Kaplan, O.I., Kida, K., Toivenon, T., Foley-Fisher, C., Cottell, D., Katada, T., Kontani, K. and Blacque, O.E. (2010) Joubert syndrome Arl13b functions at ciliary membranes and stabilizes protein transport in *Caenorhabditis elegans*. *J. Cell Biol.*, **188**, 953–969.
49. Li, Y., Wei, Q., Zhang, Y., Ling, K. and Hu, J. (2010) The small GTPases ARL-13 and ARL-3 coordinate intraflagellar transport and ciliogenesis. *J. Cell Biol.*, **189**, 1039–1051.
50. Follit, J.A., Tuft, R.A., Fogarty, K.E. and Pazour, G.J. (2006) The intraflagellar transport protein IFT20 is associated with the Golgi complex and is required for cilia assembly. *Mol. Biol. Cell*, **17**, 3781–3792.
51. Baldari, C.T. and Rosenbaum, J. (2010) Intraflagellar transport: it's not just for cilia anymore. *Curr. Opin. Cell Biol.*, **22**, 75–80.
52. Finetti, F., Paccani, S.R., Riparbelli, M.G., Giacomello, E., Perinetti, G., Pazour, G.J., Rosenbaum, J.L. and Baldari, C.T. (2009) Intraflagellar transport is required for polarized recycling of the TCR/CD3 complex to the immune synapse. *Nat. Cell Biol.*, **11**, 1332–1339.
53. Tran, P.V., Haycraft, C.J., Besschetnova, T.Y., Turbe-Doan, A., Stottmann, R.W., Herron, B.J., Chesebro, A.L., Qiu, H., Scherz, P.J., Shah, J.V. *et al.* (2008) THM1 negatively modulates mouse sonic hedgehog signal transduction and affects retrograde intraflagellar transport in cilia. *Nat. Genet.*, **40**, 403–410.
54. Shah, A.S., Farmen, S.L., Moninger, T.O., Businga, T.R., Andrews, M.P., Bugge, K., Searby, C.C., Nishimura, D., Brogden, K.A., Kline, J.N. *et al.* (2008) Loss of Bardet–Biedl syndrome proteins alters the morphology and function of motile cilia in airway epithelia. *Proc. Natl Acad. Sci. USA*, **105**, 3380–3385.
55. Gerner, M., Haribaskar, R., Putz, M., Czerwitzki, J., Walz, G. and Schafer, T. (2010) The retinitis pigmentosa GTPase regulator interacting protein 1 (RPGRIP1) links RPGR to the nephronophthisis protein network. *Kidney Int.*, **77**, 891–896.
56. Tammachote, R., Hommerding, C.J., Sinders, R.M., Miller, C.A., Czarnecki, P.G., Leightner, A.C., Salisbury, J.L., Ward, C.J., Torres, V.E., Gattone, V.H. 2nd *et al.* (2009) Ciliary and centrosomal defects associated with mutation and depletion of the Meckel syndrome genes MKS1 and MKS3. *Hum. Mol. Genet.*, **18**, 3311–3323.
57. Hurd, T.W., Gao, L., Roh, M.H., Macara, I.G. and Margolis, B. (2003) Direct interaction of two polarity complexes implicated in epithelial tight junction assembly. *Nat. Cell Biol.*, **5**, 137–142.
58. Zhou, W. and Hildebrandt, F. (2009) Molecular cloning and expression of phospholipase C epsilon 1 in zebrafish. *Gene Expr. Patterns*, **9**, 282–288.